BMC Neuroscience

BioMed Central

Research article

Human neuronal stargazin-like proteins, γ_2, γ_3 and γ_4; an investigation of their specific localization in human brain and their influence on $Ca_V2.1$ voltage-dependent calcium channels expressed in *Xenopus* oocytes.

Fraser J Moss*[1,2], Annette C Dolphin[1] and Jeffrey J Clare[3]

Address: [1]Department of Pharmacology, University College London, Gower Street, London, WC1E 6BT, UK, [2]Current address: Division of Biology, M/C 156-29, California Institute of Technology, 1200 E. California Blvd., Pasadena, CA 91125, USA and [3]Gene Expression and Protein Biochemistry, GlaxoSmithKline, Medicines Research Center, Gunnels Wood Road, Stevenage, Herts, SG1 2NY, UK

Email: Fraser J Moss* - fmoss@caltech.edu; Annette C Dolphin - a.dolphin@ucl.ac.uk; Jeffrey J Clare - jeff.j.clare@gsk.com

* Corresponding author

Published: 23 September 2003

BMC Neuroscience 2003, **4**:23

Received: 12 June 2003
Accepted: 23 September 2003

This article is available from: http://www.biomedcentral.com/1471-2202/4/23

Abstract

Background: Stargazin (γ_2) and the closely related γ_3, and γ_4 transmembrane proteins are part of a family of proteins that may act as both neuronal voltage-dependent calcium channel (VDCC) γ subunits and transmembrane α-amino-3-hydroxy-5-methyl-4-isoxazoleproponinc (AMPA) receptor regulatory proteins (TARPs). In this investigation, we examined the distribution patterns of the stargazin-like proteins γ_2, γ_3, and γ_4 in the human central nervous system (CNS). In addition, we investigated whether human γ_2 or γ_4 could modulate the electrophysiological properties of a neuronal VDCC complex transiently expressed in *Xenopus* oocytes.

Results: The mRNA encoding human γ_2 is highly expressed in cerebellum, cerebral cortex, hippocampus and thalamus, whereas γ_3 is abundant in cerebral cortex and amygdala and γ_4 in the basal ganglia. Immunohistochemical analysis of the cerebellum determined that both γ_2 and γ_4 are present in the molecular layer, particularly in Purkinje cell bodies and dendrites, but have an inverse expression pattern to one another in the dentate cerebellar nucleus. They are also detected in the interneurons of the granule cell layer though only γ_2 is clearly detected in granule cells. The hippocampus stains for γ_2 and γ_4 throughout the layers of the every CA region and the dentate gyrus, whilst γ_3 appears to be localized particularly to the pyramidal and granule cell bodies. When co-expressed in *Xenopus* oocytes with a $Ca_V2.1/\beta_4$ VDCC complex, either in the absence or presence of an $\alpha2\delta_2$ subunit, neither γ_2 nor γ_4 significantly modulated the VDCC peak current amplitude, voltage-dependence of activation or voltage-dependence of steady-state inactivation.

Conclusion: The human γ_2, γ_3 and γ_4 stargazin-like proteins are detected only in the CNS and display differential distributions among brain regions and several cell types in found in the cerebellum and hippocampus. These distribution patterns closely resemble those reported by other laboratories for the rodent orthologues of each protein. Whilst the fact that neither γ_2 nor γ_4 modulated the properties of a VDCC complex with which they could associate *in vivo* in Purkinje cells adds weight to the hypothesis that the principal role of these proteins is not as auxiliary subunits of VDCCs, it does not exclude the possibility that they play another role in VDCC function.

Background

The mutation underlying the absence epilepsy phenotype of the allelic stargazer (*stg*) and waggler (*wag*) mutant mice occurs in a gene, *cacng2*, whose product, stargazin, has been hypothesized to be a neuronal voltage dependent calcium channel (VDCC) γ subunit [1]. VDCCs are intrinsically involved in the regulation of a multiplicity of Ca^{2+} dependent processes in many different cell types where they are inserted into the plasma membrane as hetero-oligomeric complexes of a pore-forming α_1 subunit with auxiliary β, α2δ and possibly γ subunits [2].

The first VDCC γ subunit to be identified (γ_1) [3–5] was found to be solely expressed in skeletal muscle, where its function is to limit calcium entry through the L-type VDCCs of skeletal myotubes [6,7]. VDCCs purified from neuronal tissues did not appear to possess a γ subunit [8–11]. However, despite sharing only weak protein sequence identity with γ_1 (25%), stargazin (γ_2) was suggested to represent the first example of a neuronal VDCC γ subunit based on its similar tetra-spanning transmembrane structure to the γ_1 subunit and its ability to weakly modulate VDCC-current properties *in vitro* [1]. Subsequent investigations have identified six other stargazin-like genes which are currently classified as *cacng3-cacng8* (encoding proteins γ_3 - γ_8), in a continuation of the VDCC γ subunit nomenclature [12–17].

Investigation of the functional influence of these stargazin-like γ proteins upon VDCCs has yielded mixed results. Some laboratories have reported that γ_2 and its close homologue γ_4 cause small hyperpolarizing shifts in the voltage dependence of steady-state inactivation [1,14,18]. This however, might be dependent upon which other auxiliary subunits are co-expressed in the VDCC complex under investigation [18]. In contrast, Chen et al. [19] showed whole cell VDCC currents from the cerebellar granule cells of *stg* mice, which effectively lack the γ_2 subunit, do not have significantly altered voltage-dependence of activation or inactivation compared to wild type. Other laboratories reported that γ_2 or γ_3 can significantly reduce peak current amplitudes of N-type VDCCs expressed in *Xenopus* oocytes, but only when co-expressed with an $\alpha 2\delta_1$ subunit [20], and supporting this, that thalamic relay neurons from *stg* mice express enhanced low and high voltage-activated VDCC currents compared to wild type [21]. Furthermore, clear biochemical evidence has been generated for a direct interaction of γ_2 with the VDCC $Ca_V2.2$ α_1 subunit [20,22]. Another stargazin-like protein, γ_7, which is phylogenetically distinct from γ_2, γ_3 and γ_4 [13,15], almost abolishes the expression of $Ca_V2.2$ when co-expressed *in vitro*, and also reduces Ca^{2+} currents via $Ca_V1.2$ and $Ca_V2.1$ channels [15]. However, our data indicated that the influence of γ_7 on VDCC function is to reduce α_1 subunit protein expression, a functional property unlike anything reported for the other stargazin-like proteins, which suggests that γ_7 is not a subunit of a calcium channel complex [15].

Whilst controversy surrounds the role of the γ_2, γ_3 and γ_4 stargazin-like proteins in relation to VDCC modulation, a clear function has been determined for these proteins as chaperones for the appropriate trafficking and receptor biogenesis of alpha-amino-3-hydroxy-5-methylisoxazole-4-propionic acid (AMPA) receptors [19,23–25]. Consequently, these three proteins together with their close homologue γ_8, were recently dubbed transmembrane AMPA receptor regulatory proteins (TARPs) [25]. A primary interaction (probably via transmembrane and/or extracellular regions [26]) promotes the trafficking of the GluR subunits to the plasma membrane, and a secondary interaction of the C-terminus of stargazin with PSD-95 or a similar cytoskeletal protein via a PSD-95/DLG/ZO-1(PDZ)-binding motif facilitates the lateral relocation of the glutamate receptor complex to its correct position in the post-synaptic density [19] and hence influences the number of AMPA receptors located at this site [27].

Elucidation of the differential distribution of the stargazin-like proteins coupled with studies of the physiological abnormalities underlying the epilepsy phenotypes of the mice expressing what are effectively null mutations of γ_2 has also helped to determine some of the normal functions of these proteins in the murine CNS. The *stg* and *wag* mice display a loss of the fast component of EPSC at mossy fiber to cerebellar granule cell synapses [28,29], plus reduced synaptic transmission at parallel fiber Purkinje cell synapses in *wag* [29]. However, the synaptic transmission to CA1 pyramidal cells (Schaffer collateral projection) in *stg* is not altered [28]. *In situ* hybridization studies have determined that murine γ_2 is normally expressed at its highest levels in the cerebellum [1,14,19]. γ_3 and γ_4 mRNAs are also detected in mouse cerebellum but γ_3 mRNA has been detected only in the Golgi neurons of the granule cell layer and is absent from the molecular layer [19]. γ_4 mRNA is localized to the Purkinje, rather than the granule cell layer [14]. Whilst this manuscript was in preparation, Tomita et al. [25] reported that γ_2 is the only TARP expressed in rat cerebellar granule cells, but like mouse, all isoforms are detected in hippocampus [1,14,19,25]. The genetic defect in *stg* results in the loss of γ_2 mRNA and protein and does not appear to result in up- or down-regulated expression of γ_3 or γ_4 [1,22]. Collectively, these data suggest that *stg* mice exhibit the loss of fast synaptic transmission in the mossy fiber to granule cell synapse because γ_2 is the major and possibly the only stargazin-like protein in the cerebellar granule cells of wild-type mice and no other stargazin-like protein is expressed at sufficient levels to rescue normal AMPA receptor trafficking and maturation. The reason that

synaptic transmission to CA1 pyramidal cells in *stg* mice is preserved is probably because, although γ_2 is not expressed in *stg*, the total remaining TARP expression levels in hippocampal CA1 pyramidal cells are adequate to promote normal surface expression of mature AMPA receptors at the postsynaptic membrane in this synapse.

It was therefore of great interest to examine whether the expression patterns of the human stargazin-like proteins paralleled those of mouse and if they were differentially expressed in the various cell types of each tissue. This study presents the differential distribution of γ_2, γ_3 and γ_4 in human brain by northern blotting and more detailed immunohistochemical analysis of their expression in human cerebellum and hippocampus. In addition, we used the results of our distribution study to investigate whether the human γ_2 and γ_4 could modulate currents gated by a VDCC complex heterologously expressed in *Xenopus* oocytes that was assembled from the major VDCC subunits expressed in a cerebellar Purkinje cell.

Results

Northern Blot analysis of mRNA distribution

The overall tissue distribution of human γ_2, γ_3 and γ_4 mRNAs was analyzed by northern blotting. Specific cDNA probes representing each gene were generated as described in the methods and hybridized against a human multiple-tissue northern blot (Figure 1A) and two brain region blots (Figure 1B and 1C). The γ_2-specific cDNA probe detected two mRNAs of approximately 7 kb and 3 kb. Bands of similar size were reported in a mouse multiple-tissue blot probed with a murine γ_2 cDNA probe [1]. Like mouse, the human γ_2 mRNA transcripts were detected only in brain (Figure 1A), and were particularly abundant in cerebellum, cerebral cortex, occipital lobe, frontal lobe and temporal lobe, hippocampus and thalamus (Figure 1B and 1C). γ_2 transcripts were detected at somewhat lower levels in medulla, putamen, amygdala and substantia nigra but only weakly in caudate nucleus. γ_2 transcripts were absent from corpus callosum and the sub-thalamic nucleus and spinal cord.

A γ_3 cDNA probe detected one 2.0–2.1 kb γ_3 mRNA transcript which like γ_2, was exclusively localized to the brain (Figure 1A). However, γ_3 mRNA was detected only in cerebral cortex, including occipital lobe, frontal lobe, and temporal lobe, the putamen, caudate nucleus, amygdala and hippocampus and was absent from all of the other regions probed (Figure 1B and 1C).

The γ_4-specific probe identified an mRNA of approximately 4 kb detected exclusively in brain (Figure 1A). This was widely detected throughout the brain but was most prevalent in the putamen and caudate nucleus. Unlike γ_2 or γ_3, γ_4 mRNA was also weakly detected in spinal cord.

Generation and characterization of γ specific antisera

In order to investigate the distribution of the γ_2, γ_3 and γ_4 proteins and to analyze their expression in different neuronal cell types we generated specific antisera against each isoform. These were generated using peptide immunogens that were selected to be subtype-specific as determined by multiple sequence alignment. To confirm activity against the corresponding holopeptide and lack of cross-reactivity with the other subtypes, each of these antisera were validated against the different subunit proteins recombinantly expressed in COS-7 cells. Cells were transiently transfected with a pMT2 expression vector containing either the human γ_2, γ_3 or γ_4 cDNAs, and 2–3 days later were analyzed by immunocytochemistry. All three γ isoforms could be readily detected and were localized largely in the plasma membrane of the cells (Figure 2A). The specificity of the antibodies (Abs) was confirmed by incubating non-transfected cells with each primary Ab, which in each case gave no immunoreactivity (Figure 2B). Similar results were obtained when cells expressing one of the γ isoforms were incubated with Abs directed against either of the other two γ proteins (data not shown). Cells transfected with a γ cDNA but which were not permeablized after fixation also exhibited no immunoreactivity (Figure 2C). Since the peptide sequences chosen for immunization are in the C-terminus, these results indicate this portion of recombinantly expressed γ_2, γ_3 and γ_4 is located intracellularly. Co-transfection of VDCC subunits $Ca_V2.1$ and β_4 did not alter the expression pattern of the γ proteins indicating that there are no effects on trafficking and that the anti-γ Abs did not cross-react with the $Ca_V2.1$ or β_4 subunits (data not shown).

Immunolocalization of γ_2, γ_3 and γ_4 in human cerebellum and hippocampus

Immunohistochemical analysis was carried out to examine the differential expression of γ_2, γ_3 and γ_4 in human cerebellum and hippocampus. Control experiments to measure non-specific binding to tissue sections were performed by pre-absorbing antisera overnight with 100 μM of the relevant peptide (Figures 3E and 3I, 4C and 4D, 5C and 5D and 6B) and by omitting the primary antibody (data not shown).

Cerebellum

Figure 3 shows the pattern of staining observed in the cerebellum using γ_2, γ_3 and γ_4 specific antisera. Moderate γ_2-specific staining was seen in the molecular layer suggesting expression in the dendrites of cerebellar Purkinje neurons (Figure 3A). Small cell bodies in the molecular layer that were most likely stellate or basket cell interneurons also stained positively. The γ_2 immunostaining was also strong in the soma of Purkinje neurons extending to the dendrites, but decreasing in intensity following the first few bifurcations (Figure 3A). Cerebellar granule cells were

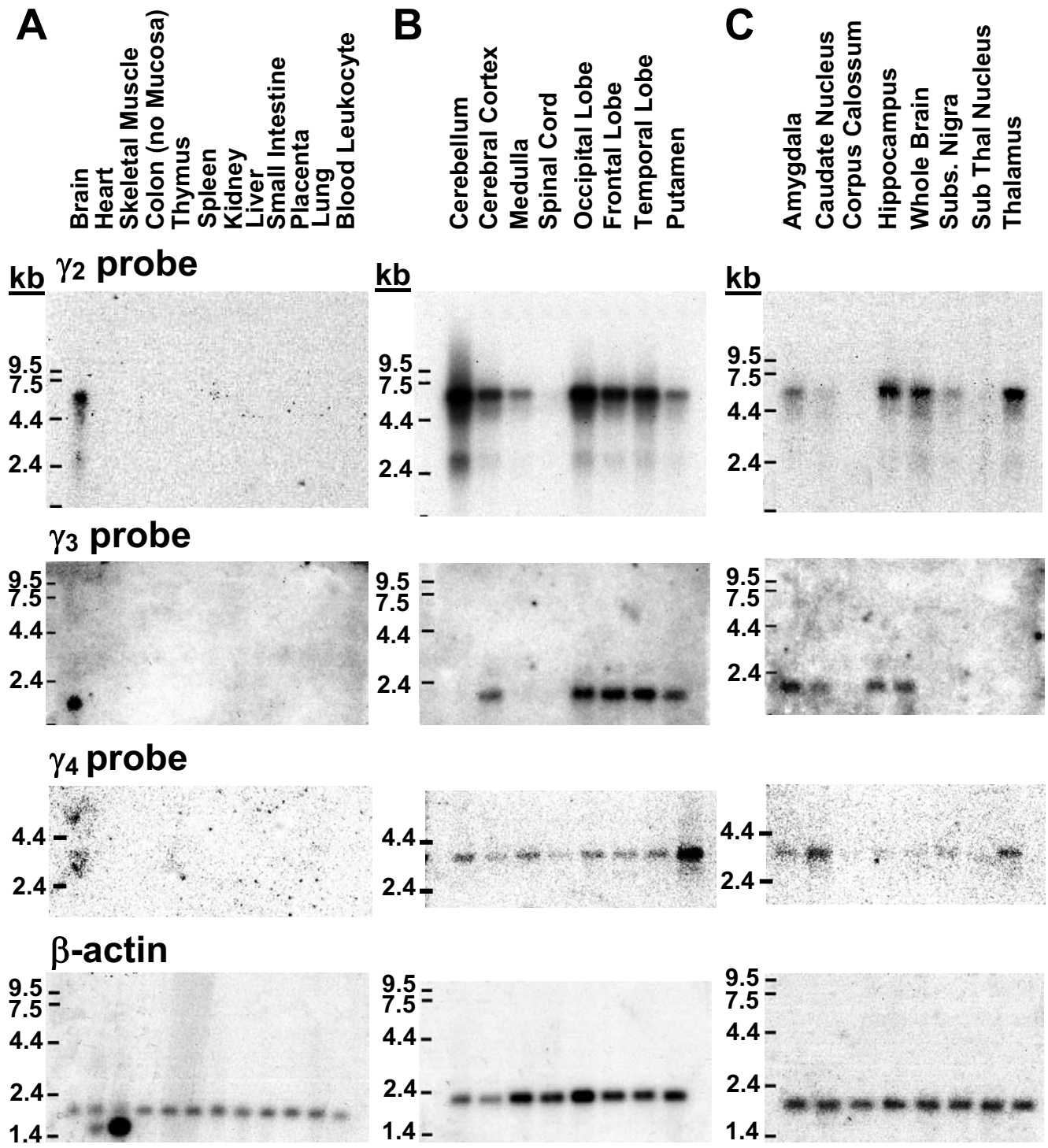

Figure 1

Northern blot analysis of the human γ_2, γ_3, and γ_4 mRNA transcripts. A. Human multiple-tissue northern blots revealed that the γ_2, γ_3, and γ_4 are exclusively detected in the brain. **B & C**. Brain region blots determined that the γ_2 and γ_4 are almost ubiquitously expressed, but at differential levels in the same tissues. γ_3 is more specifically localized to cerebral cortex, amygdala, caudate nucleus and hippocampus. Size markers were from an RNA ladder provided on the blot by BD Biosciences Clontech and the β-actin control probe results are displayed in the bottom panels.

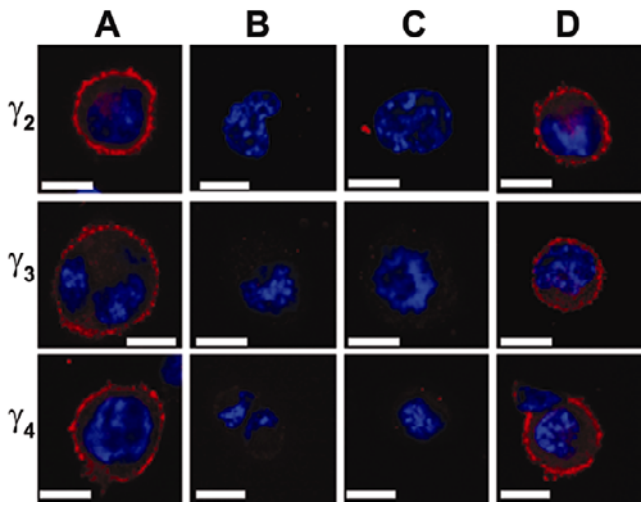

Figure 2
Transient expression of γ_2, γ_3, and γ_4 in COS-7 cells. A. Positive staining for γ_2, γ_3, or γ_4 (red) is strongly localized to the membranes of permeablized cells transfected with the individual γ_2, γ_3, or γ_4 cDNAs. Little immunostaining is observed in the cytoplasm between the membrane and nucleus (blue). **B.** Non-transfected cells did not stain for γ_2, γ_3, or γ_4 using the Abs generated in this study. **C**. Cells transfected with γ_2, γ_3, or γ_4 cDNA, but not permeablized during the staining process do not show immunoreactivity for the appropriate anti-γ Abs. **D**. When co-transfected together with the $Ca_V2.1$ and β_4 VDCC subunit cDNAs, the expression patterns of γ_2, γ_3, or γ_4 were unaltered. Scale bars in all panels represent 10 μm.

moderately stained for γ_2 (Figure 3B), although assessment of immunostaining in this cell type was difficult since the majority of cell volume is comprised of the nucleus. The strongest γ_2 immunostaining in this region was actually in the interneurons. Figure 3C shows strong γ_2 immunostaining in the cell bodies of the dentate cerebellar nucleus with only weak to moderate staining in the surrounding neuropil.

Very weak γ_3 staining was observed in Purkinje cell bodies and in the interneurons of the granule cell layer (Figure 3D). Staining of the molecular layer neuropil and the granule cells is comparable to the peptide pre-absorption control (Figure 3E). It is therefore possible that the γ_3 protein is poorly represented in these particular cell types and not completely absent from the cerebellum. No γ_3 immunoreactivity was observed in the dentate cerebellar nucleus (data not shown).

Staining of a human cerebellar folium for γ_4 is shown in Figure 3F. The molecular layer and adjacent granule cell layer was lightly to moderately stained, but the staining of the Purkinje cell bodies and dendrites was striking. γ_4 immunostaining extended well into the Purkinje cell dendritic arbors from the cell body indicating that γ_4 expressed well throughout this cell type. The cell bodies that stained positively in the molecular layer were small interneurons. In the granule cell layer the interneurons stained strongly for γ_4 whereas the granule cells appear unstained (Figure 3G). In the dentate cerebellar nucleus (Figure 3H), γ_4 immunostaining was detected strongly in the perisomatic neuropil with only weak staining in the cell bodies. Interestingly, this staining pattern was almost the complete inverse of the γ_2 immunostaining in the same region (Figure 3C).

Hippocampus and dentate gyrus

Immunohistochemistry revealed differential expression patterns for γ_2, γ_3 and γ_4 in the different regions and cell types of human hippocampus and dentate gyrus (Figure 4, 5 and 6). When incubated with the anti-γ_2 Ab, generalized staining of the cell layers and neuropil throughout the hippocampal formation was observed. In Figure 4A the alveus, stratum oriens most adjacent to the CA1 pyramidal layer, and the pyramidal layer all stained moderately for γ_2. The stratum radiatum and lacunosum-moleculare stained much more weakly. The CA2 and CA3 pyramidal layers stain well for the γ_2 subunit (Figure 4B) and the intensity of staining in the alveus increased slightly in this region. It is however apparent that there is only a very weak staining of the strata oriens and radiatum in the CA2/3 regions; yet, moderate immunostaining is detected in the stratum lucidum. Weak staining is visible in the stratum lacunosum-moleculare. In the same section we also observed moderate γ_2 staining in the molecular layer of the dentate gyrus and strong immunostaining in the granule cells (examined at higher magnification on Figure 4H). The γ_2 staining was weak or absent in the polymorphic layer, but distinct fibers were stained which course across this region. Moderate staining of cell bodies in CA4 was also observed (Figure 4B, top left portion of the panel). Pre-absorption controls using the γ_2 peptide immunogen (Figures 4C and 4D) show the background staining in a serial section of the same hippocampus as in Figures 4A and 4B. The perisomatic staining in the stratum pyramidale, in the region of the CA1 towards the CA2 was moderate, with slightly more intense somatic staining (Figure 4E). An apparently higher level of γ_2 staining in the CA2 and CA3 regions (Figures 4F and 4G) compared to CA1 was probably due to a higher density of pyramidal cell soma in these regions compared to the CA1 region [30].

Staining for γ_3 was absent from the alveus, stratum oriens, stratum radiatum and lacunosum-moleculare, but the pyramidal layer of the CA1, CA2 and CA3 regions of

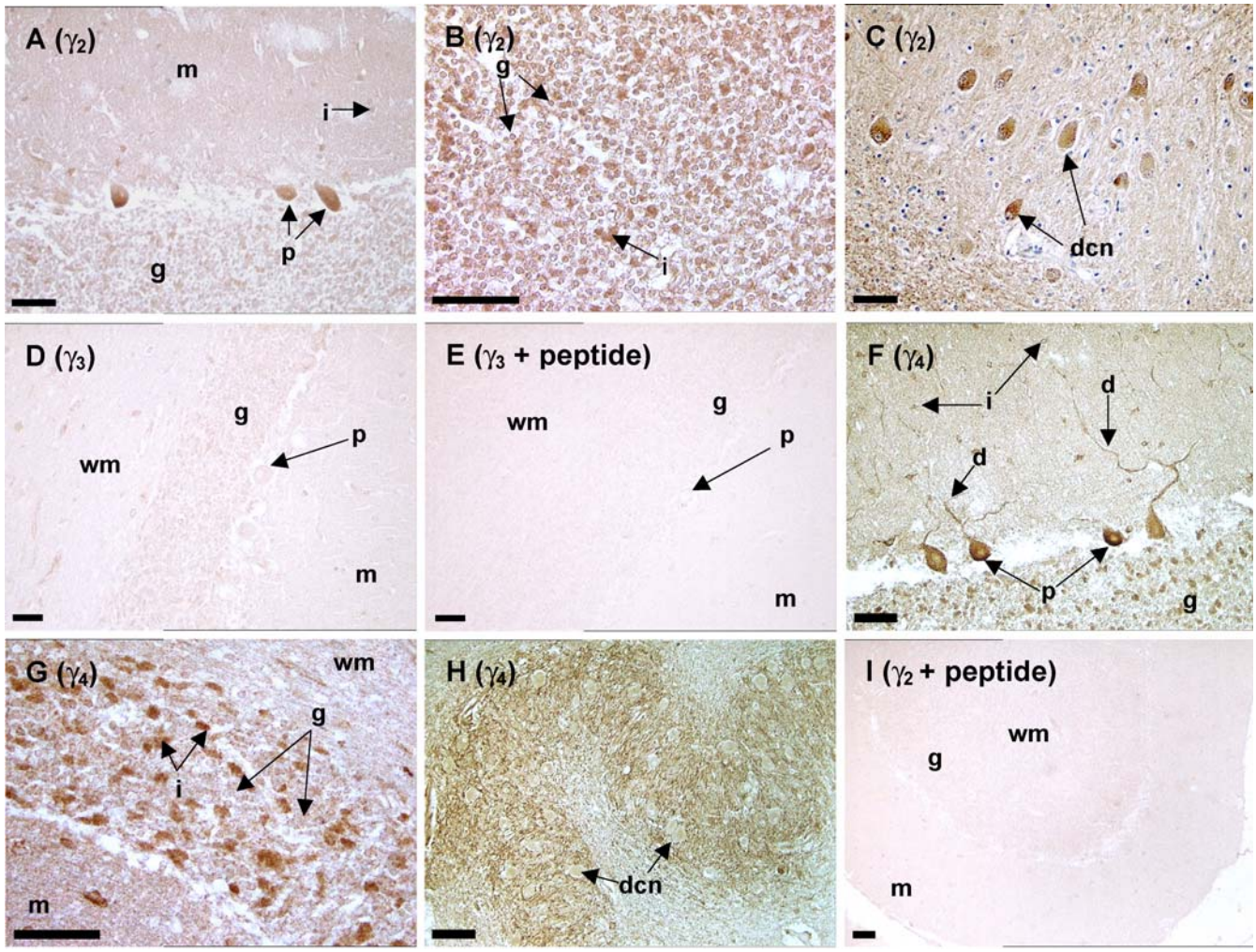

Figure 3

Expression of the γ_2, γ_3, and γ_4 stargazin-like proteins in human cerebellum. A. γ_2 immunoreactivity in the molecular layer (**m**) and part of the adjacent granule cell layer (**g**) in a cerebellar folium. Strong γ_2 immunostaining was seen in the Purkinje cell somata (**p**) that continued into the dendrites, observed as moderate staining of the molecular layer neuropil. Cell bodies in the molecular layer with positive γ_2 immunoreactivity are small interneurons (**i**). **B.** In the granule cell layer, the granule cells (**g**) are moderately stained for γ_2 although the strongest immunostaining in this region is actually in the interneurons (**i**). **C.** The dentate cerebellar nucleus (**dcn**), displayed strong γ_2 immunostaining in the cell bodies of this nucleus with only weak to moderate staining in the surrounding neuropil. In this particular section, cell nuclei are stained blue by Mayer's hematoxylin counterstain. **D.** Cerebellar folia displayed little to no γ_3 immunostaining in the central white matter (**wm**) and molecular layer (**m**). Weak immunostaining was observed in the Purkinje cell bodies and the interneurons of the granule cell layer (**g**). **E**. Pre-absorption control, with the peptide immunogen for the γ_3 Ab in the adjacent section to Fig. **3D**. **F**. The cell bodies of the Purkinje cells (**p**) stained strongly for γ_4 and this extended well into the Purkinje cell dendrites (**d**). The surrounding molecular layer neuropil (**m**) displayed light-moderate staining, as did the granule cell layer (**g**). Cell bodies in the molecular layer immunoreactive to the γ_4 Ab were small interneurons (**i**). **G.** Granule cell layer interneurons (**i**) stained much more strongly for γ_4 than the granule cells (**g**). **H.** The dcn gave a strong γ_4 immunostaining signal in the perisomatic neuropil with only weak staining in the nucleus cell bodies. **I.** Immunizing peptide pre-absorption control for the γ_2 Ab. Pre-absorption of the γ_3 or γ_4 Abs with their immunizing peptides produced almost identical results. Scale bars in all panels represent 25 μm.

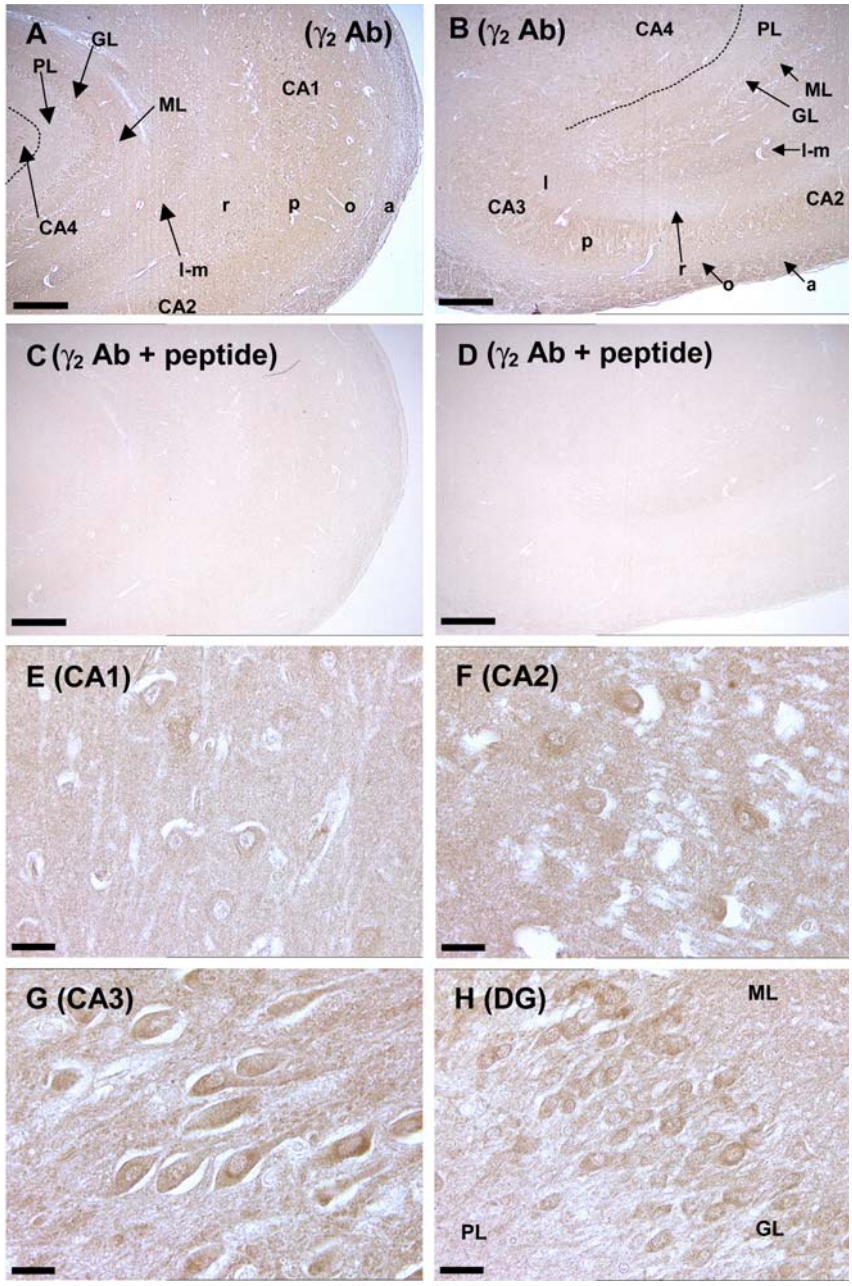

Figure 4

γ_2 immunohistochemistry in human hippocampus. A. In the CA1, alveus (**a**), stratum oriens (**o**) most adjacent to the pyramidal layer, and the pyramidal layer (**p**) all stain moderately for γ_2. The stratum radiatum (**r**) and lacunosum-moleculare (**l-m**) stain much more weakly. **B**. Strong detection of γ_2 protein occurred in the alveus and pyramidal layers of CA2 and CA3 regions. Moderate immunostaining is detected in stratum lucidum (**l**). Staining of the strata oriens and radiatum was very weak in this region. The dentate gyrus molecular layer (**ML**) stains moderately for γ_2 and the granule layer strongly (**GL**). γ_2 staining is weak or absent in the polymorphic layer (**PL**). Cells in the CA4 show moderate staining. **C and D**. Serial sections to those displayed in panels **A** and **B** incubated with synthesis peptide pre-absorbed γ_2 Ab. **E**. In the region of the CA1 towards the CA2 the perisomatic staining is light to moderate with similar staining of the cell bodies. **F**. In the CA2, staining of neuropil and cell bodies is more intense than in CA1. **G**. Staining of the soma of the CA3 hippocampal neurons is strong with moderate staining of the surrounding neuropil. **H**. The dentate gyrus shows moderate staining of the molecular layer and dense immunostaining in the granule layer. The polymorphic layer is weakly stained. Scale bar in panels **A–D** represents 250 μm, in panels **E–H** 25 μm. The dotted lines in panels **A** and **B** represent the border between the CA4 region of the hippocampus and the polymorphic layer of the dentate gyrus.

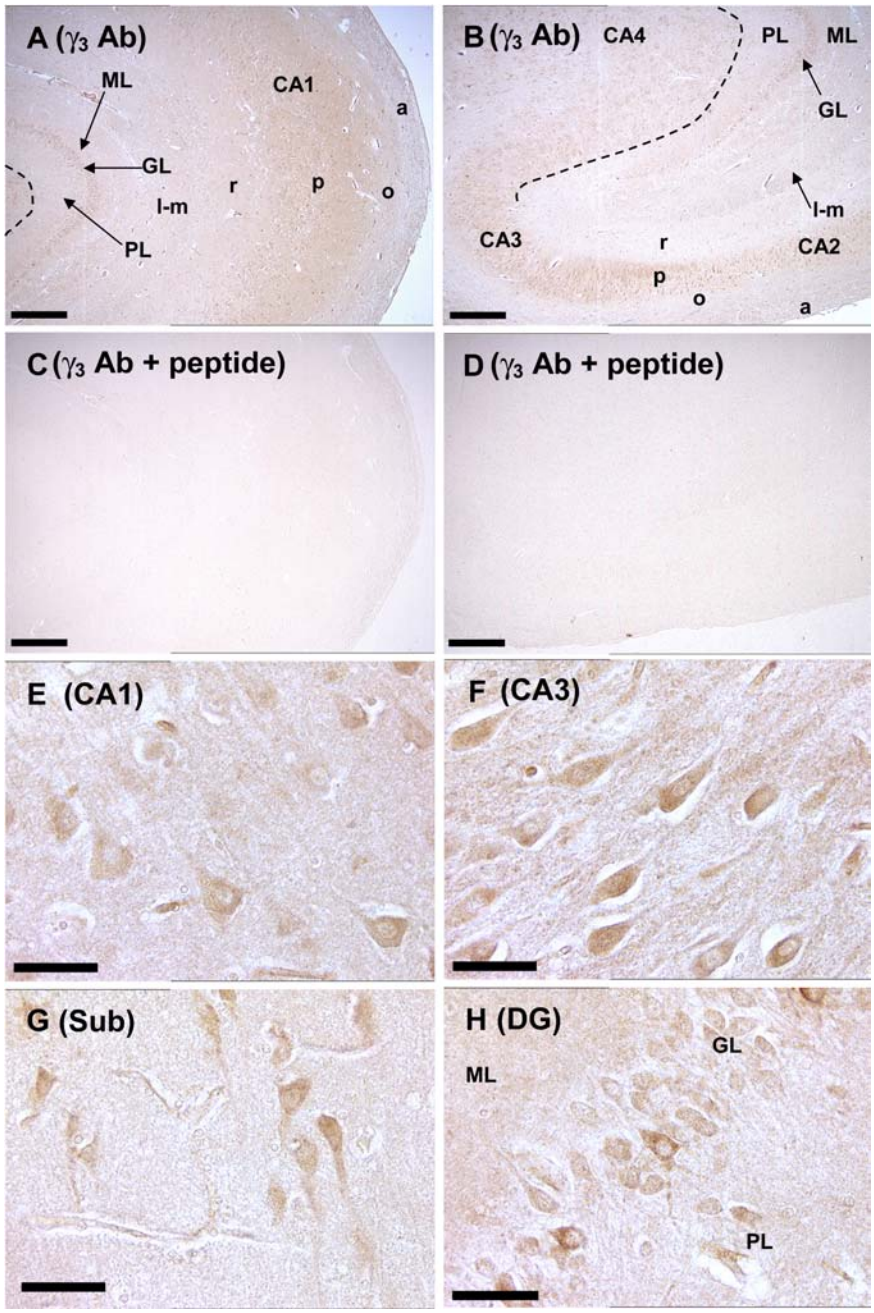

Figure 5

γ_3 immunohistochemistry in human hippocampus. A. The pyramidal cell layer (**p**) of the CA1 region exhibited moderate to strong staining for γ_3. Weak staining was observed in the stratum oriens (**o**) and stratum radiatum (**r**). The alveus (**a**) and lacunosum-moleculare (**l–m**) are in general, absent of immunoreactivity. **B**. More intense γ_3 immunostaining was observed in the CA2 and CA3 pyramidal cell layers than in CA1. Strong staining was also detected in CA4 cell bodies but surrounding neuropil is devoid of immunoreactivity. **C and D**. Sections adjacent to those displayed in panels **A** and **B** incubated with immunizing peptide-pre-absorbed γ_3 Ab. **E**. Moderate to strong staining of CA1 pyramidal cell bodies and weaker staining in the surrounding neuropil. **F**. Intense staining of the pyramidal cells of the CA3 with moderate perisomatic staining. **G**. Cell bodies in the subiculum (**Sub**) are moderately stained and neuropil staining is very weak. Neuropil staining in panels **E**, **F** and **G** may reflect relative cell densities in each region. **H**. Granule cells of the dentate gyrus were stained moderately to strongly by the γ_3 Ab. The immunoreactivity is mainly in the soma of these cells, but can also be seen in the early branches of the granule cells dendritic trees, which extend into the lightly stained molecular layer. The neuropil of the polymorphic layer is almost devoid of staining. Scale bars in panel **A–D** represent 250 μm, in panels **E–H** 25 μm.

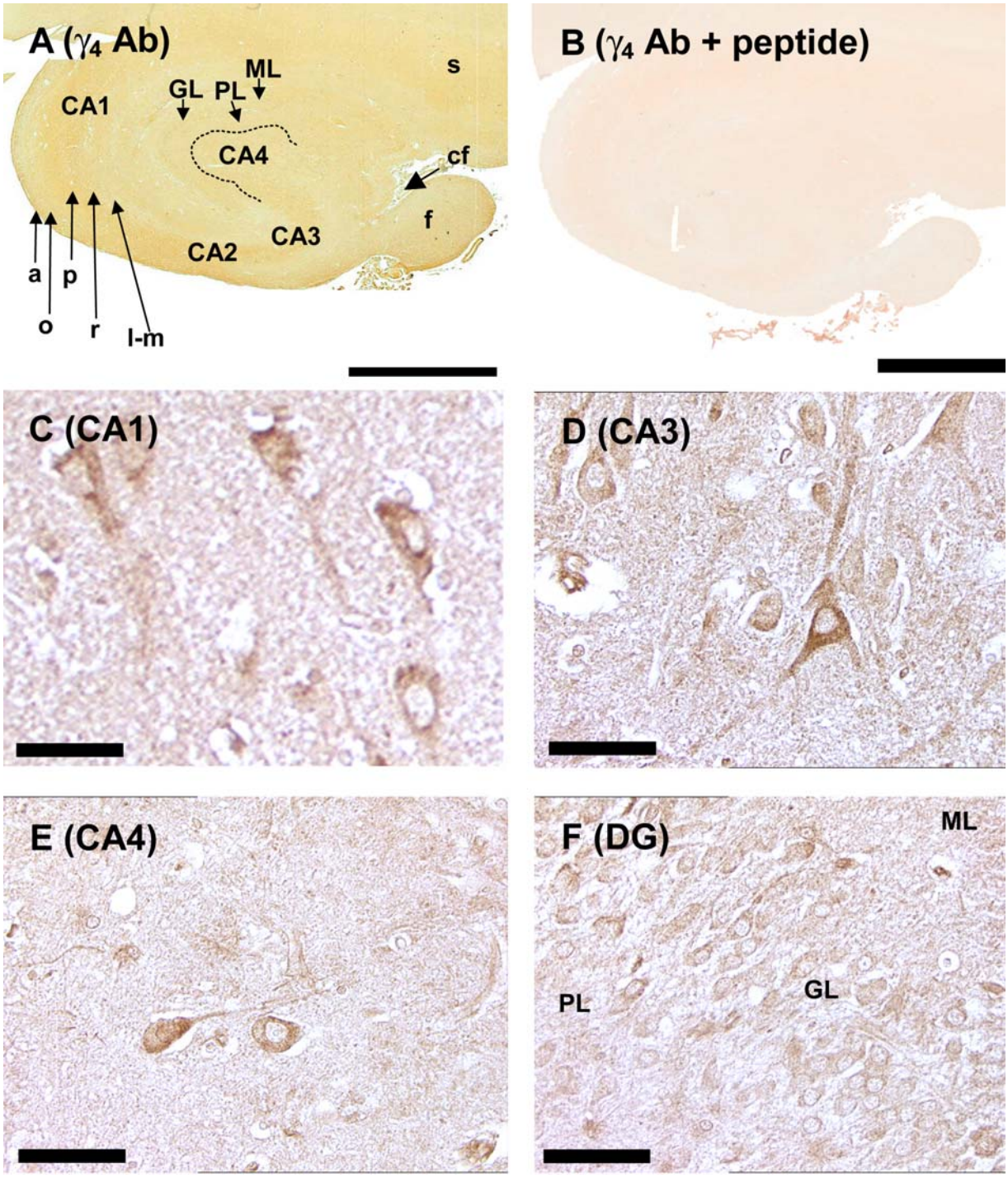

Figure 6

γ_4 immunohistochemistry in human hippocampus. A. γ_4 immunoreactivity was seen throughout the pyramidal cell layers each region of Ammon's horn and the surrounding neuropil with staining most intense in the CA2/3 transition region. Labeled regions are as in figures 4 and 5 with the addition of subiculum (**s**) choroidal fissure (**cf**) and fimbria (**f**). **B**. Section adjacent to that in panel **A** incubated with immunizing peptide pre-absorbed γ_4 Ab. **C**. CA1 pyramidal cell bodies are moderately to strongly stained by γ_4 Ab with moderate staining in surrounding neuropil. **D**. Strong staining of pyramidal cells in the CA3 with only slightly weaker immunostaining in the neuropil. **E**. Staining of CA4 cell bodies is moderate to strong with moderate neuropil staining. **F**. Although positively stained, the granule neurons of the dentate gyrus do not stain as strongly for γ_4 as do pyramidal cells. Scale bars in panel **A** and **B** represent 5 mm and in panels **C–F** 25 μm.

Ammon's horn strained strongly, with lesser immunostaining in the subiculum and CA4 regions (Figure 5A and 5B). Closer examination revealed that the pyramidal cell bodies stained strongly for γ_3 and this staining was strongest in CA3 and became progressively weaker through the CA2 and CA1 regions and into the subiculum. High power images of CA1 (Figure 5E), CA3 (Figure 5F), and subiculum (Figure 5G) determined that this was most likely to be caused by increased cell densities in the CA2/3 regions rather than more intense staining of pyramidal neurons, although perisomatic staining was more intense in the CA3 region than CA1, and absent from the subiculum. Visible in Figure 5A and 5B, and also observed at an increased magnification in Figure 5H, the granule layer of the dentate gyrus is distinctly labeled whereas the molecular and polymorphic layers display weak or no immunostaining. The granule cells stained moderately to strongly for γ_3 and the immunoreactivity was mainly in the soma of these cells, but could also be seen in the early branches of the granule cell dendritic trees, which extend into the lightly stained molecular layer (Figure 5H).

At the macroscopic level, medium to strong γ_4 immunostaining was seen throughout the pyramidal layers of Ammon's horn and in the alveus (Figure 6A). The alveus stained strongly for γ_4 as did the cell bodies in the pyramidal layer of all CA regions. This was observed more clearly at high power with a similar high level of staining of pyramidal cell bodies throughout the CA1-4 regions, but with the most intense perisomatic staining observed in the CA2/3 region (Figure, 6C, 6D, and 6E). Weak to moderate staining was observed throughout the neuropil of the strata surrounding the pyramidal layers in all regions. In the dentate gyrus, the granule cell layer appears to stain slightly more strongly than the adjacent molecular or polymorphic regions (Figure 6F). This also may be an artifact of the cell density in the granule layer rather than increased expression of the γ_4 protein in the dentate granule cell bodies compared to their processes.

The effects of γ_2 and γ_4 on the biophysical properties of $Ca_V2.1$ calcium channels

Since the role of the stargazin-like proteins in relation to VDCC function remains controversial we examined the effects of γ_2 and γ_4 on the biophysical properties of $Ca_V2.1$ calcium channels. Together with the $Ca_V2.1$ α subunit, we co-expressed a β_4 subunit with or without an $\alpha2\delta_2$ subunit. These VDCC subunits are known to be highly expressed in cerebellar Purkinje cells [31–38], a cell type that, according to the immunohistochemistry data presented herein, strongly expresses both γ_2 and γ_4. Figure 7A and 7B show the current-voltage relations of $Ca_V2.1/\beta_4$ and $Ca_V2.1/\beta_4/\alpha2\delta_2$ VDCCs respectively, expressed in *Xenopus* oocytes either in the presence or absence of γ_2 or γ_4. Neither γ_2 nor γ_4 produced a statistically significant shift in the half-maximal voltage of activation (V_{50act}) of $Ca_V2.1/\beta_4$ (Table 1). The slope factor (k_{act}), maximum conductance (G_{max}), and peak current amplitude at +10 mV were also very similar to controls on co-expression of either γ_2 or γ_4 in the absence the $\alpha2\delta_2$ subunit. Co-expression of the $\alpha2\delta_2$ subunit was sufficient to significantly increase the G_{max} and peak current amplitude of a $Ca_V2.1/\beta_4$ Ca^{2+} channel complex (Figure 7A and 7B). However, the increase was not affected by the additional co-expression of either γ_2 or γ_4.

No statistically significant differences were observed in the half-maximal voltage of steady-state inactivation ($V_{50inact}$) or slope factor (k_{inact}) of $Ca_V2.1/\beta_4$ or $Ca_V2.1/\beta_4/\alpha2\delta_2$ VDCCs co-expressing γ_2 or γ_4 (Figure 7C, 7D and 7E and Table 2).

Discussion

Differential distribution of human stargazin-like γ mRNAs

The northern blot analysis described herein detected the human γ_2, γ_3 and γ_4 mRNAs only in the brain. Similar mRNA distributions and transcript sizes have been reported by *in situ* hybridization and northern blot for the mouse orthologues [1,14,19] and these data are supported by western blots [22]. We do not however rule out the possibility that human γ_2, γ_3 and γ_4 may be expressed in some non-CNS tissues that are not included on the multiple tissue northern blot used in this study. Other laboratories that employed highly sensitive reverse-transcriptase polymerase chain reaction expression analyses have reported that γ_4 in particular is expressed in some non-neuronal tissues [13,17]. The γ_2 and γ_4 transcripts were detected in most of the brain regions probed and mainly in the same tissues. However, in some regions where both isoforms are detected, for example the cerebellum or thalamus, γ_2 expression is higher than γ_4, whereas in the basal ganglia regions of putamen and caudate nucleus γ_4 mRNA is the more highly represented transcript. γ_3 is much more selectively detected, but its expression is coincident with both γ_2 and γ_4 in all regions in which it was detected by northern blot.

An additional observation was that these stargazin-like γ proteins are differentially detected in some of the nuclei that comprise the basal ganglia, a region believed to be involved in the planning and programming of movement, or more broadly in the processes by which intention is converted into voluntary action. The putamen has a heterogeneous neuronal γ population with γ_4 mRNA possibly the most prevalent of the three γ transcripts investigated herein, as has been previously observed in both mouse and rat brain [14,25]. The caudate nucleus also expresses transcripts for all three stargazin-like γ proteins, however the signal detected with the γ_2 probe was extremely weak

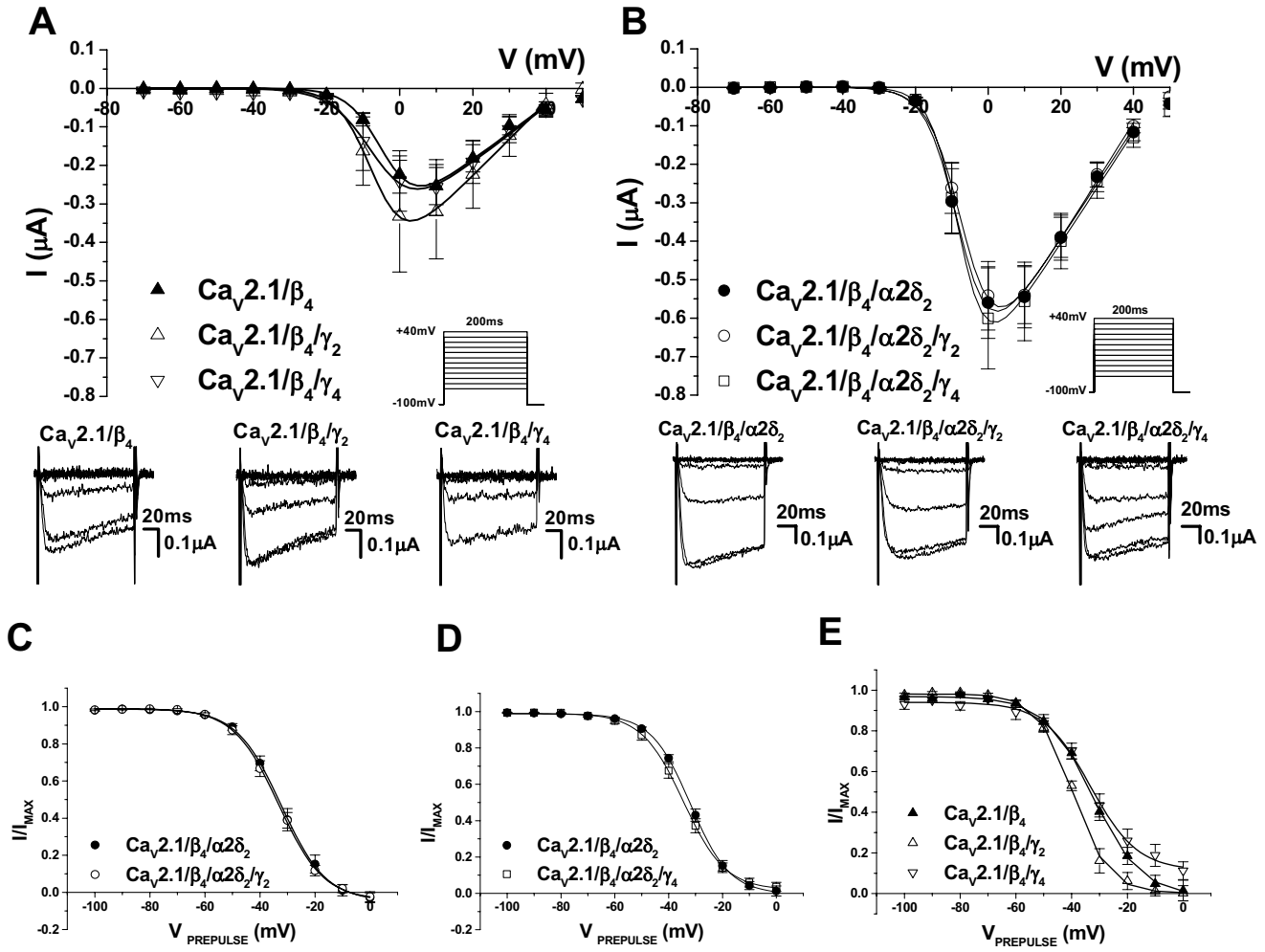

Figure 7

Influence of γ_2 and γ_4 upon Ca_V 2.1/β_4 ± $\alpha2\delta_2$ VDCC currents expressed in *Xenopus* oocytes.A The peak current-voltage relationships for $Ca_V2.1/\beta_4$ (n = 16), $Ca_V2.1/\beta_4/\gamma_2$ (n = 14) and $Ca_V2.1/\beta_4/\gamma_4$ (n = 11) show no significant differences in any parameters (Table 1). The bottom panels display representative traces recorded from a single oocyte injected with each subunit combination investigated. **B**. The peak current-voltage relationships for $Ca_V2.1/\beta_4/\alpha2\delta_2$ (n = 43), $Ca_V2.1/\beta_4/\alpha2\delta_2/\gamma_2$ (n = 34) and $Ca_V2.1/\beta_4/\alpha2\delta_2/\gamma_4$ (n = 20) show no significant differences in any parameters (Table 1). In both panels **A** and **B**, only representative traces from -50 to +10 mV are displayed for reasons of clarity. **C**. Mean steady state inactivation data for I_{Ba} recorded in 10 mM Ba^{2+} from *Xenopus* oocytes injected with $Ca_V2.1/\beta_4/\alpha2\delta_2$ (n = 18) or $Ca_V2.1/\beta_4/\alpha2\delta\gamma$ (n = 18) **D**. $Ca_V2.1/\beta_4/\alpha2\delta_2$ (n = 20), or $Ca_V2.1/\beta_4/\alpha2\delta_2/\gamma_4$ (n = 20). Co-expression of either γ_2 or γ_4 produced data almost identical to the control. **E**. Oocytes injected with $Ca_V2.1/\beta_4$ (n = 22), $Ca_V2.1/\beta_4\gamma_2$ (n = 16) and $Ca_V2.1/\beta_4\gamma_4$ (n = 9) normalized to the maximum current I_{max} and fitted with a single Boltzmann function. The numerical data for parameters defining the steady-state inactivation relationships are displayed in Table 2.

in comparison to those for γ_3 and γ_4. On the other hand, γ_2 was the most prevalent species detected in substantia nigra, with faint detection of γ_4 and no γ_3 signal. No signals for any of the γ transcripts were detected in the subthalamic nucleus. Further immunohistochemical and electrophysiological investigation will be required to elucidate why γ_2, γ_3 and γ_4 have such differential distributions in these nuclei.

In vitro expression of human stargazin-like proteins and antibody specificity

The transient expression of cloned human γ_2, γ_3 and γ_4 cDNAs in COS-7 cells served several purposes: It deter-

Table 1: Characteristics of I_{Ba} via $Ca_V2.1/\beta_4$ or $Ca_V2.1/\beta_4/\alpha2\delta_2$ with or without γ_2 or γ_4

Channel	Activation				n
	$V_{0.5act}$(mV)	$k_{act.}$	G_{max} (μS)	Peak at +10 mV (μA)	
$Ca_V2.1/\beta_4$	-2.60 ± 0.65	5.39 ± 0.49	8.45 ± 2.20	-0.25 ± 0.05	16
$Ca_V2.1/\beta_4/\gamma_2$	-4.27 ± 1.24	4.91 ± 0.52	9.96 ± 3.34	-0.32 ± 0.12	14
$Ca_V2.1/\beta_4/\gamma_4$	-5.70 ± 2.26	5.43 ± 0.47	8.16 ± 2.59	-0.26 ± 0.07	11
$Ca_V2.1/\beta_4/\alpha2\delta_2$	-4.60 ± 0.59	4.03 ± 0.15	14.97 ± 2.05 *	-0.54 ± 0.08	43
$Ca_V2.1/\beta_4/\alpha2\delta_2/\gamma_2$	-4.13 ± 0.63	4.46 ± 0.14	15.43 ± 1.96	-0.54 ± 0.07	34
$Ca_V2.1/\beta_4/\alpha2\delta_2/\gamma_4$	-5.56 ± 0.60	3.96 ± 0.24	14.8 ± 2.64	-0.56 ± 0.10	20

To analyze the voltage-dependent activation, current-voltage (I-V) relationships (Figure 7A and Figure 7B) were fitted with a modified Boltzmann equation (see methods) to calculate V_{50act}, the mid-point of voltage dependence of activation, k_{act}, the slopefactor and G_{max}, the maximum conductance. Values are expressed as mean ± S. E. M. of the number of replicates, n. One-way analysis of variance (ANOVA) tests determined no statistically significant changes in any pairs of data differing by the presence of a γ_2 or γ_4 $P < 0.05$ was considered significant). Statistically significant differences observed between the $Ca_V2.1/\beta_4$ and $Ca_V2.1/\beta_4/\alpha2\delta_2$ channels are indicated by * ($P < 0.05$).

Table 2: Steady state inactivation properties of $Ca_V2.1/\beta_4$ or $Ca_V2.1/\beta_4/\alpha2\delta_2$ with or without γ_2 or γ_4

Channel	Inactivation		n
	$V_{50inact}$ (mV)	k_{inact}	
$Ca_V2.1/\beta_4/\alpha2\delta_2$	-31.52 ± 1.58	7.04 ± 0.19	18
$Ca_V2.1/\beta_4/\alpha2\delta_2/\gamma_2$	-33.44 ± 1.49	7.10 ± 0.23	18
$Ca_V2.1/\beta_4/\alpha2\delta_2$	-31.40 ± 0.89	7.04 ± 0.28	20
$Ca_V2.1/\beta_4/\alpha2\delta_2/\gamma_4$	-34.60 ± 1.43	6.61 ± 0.28	20
$Ca_V2.1/\beta_4$	-32.40 ± 1.09	8.43 ± 0.61	22
$Ca_V2.1/\beta_4/\gamma_2$	-37.30 ± 1.75	7.52 ± 0.74	16
$Ca_V2.1/\beta_4/\gamma_4$	-31.50 ± 1.80	8.40 ± 0.92	9

Steady-state inactivation data from Figures 7C, 7D and 7E were fitted with a single Boltzmann function (see methods). Values are expressed as mean ± S. E. M. of the number of replicates, n. In the presence of an $\alpha2\delta_2$ subunit, neither γ_2 nor γ_4 caused statistically significant modulation of the measured parameters according to an un-paired Student's *t*-test ($P < 0.05$ was considered significant). Equally, when the $\alpha2\delta_2$ subunit was omitted from the injection mixture, ANOVA determined no statistically significant changes in any pairs of data differing by the presence of a γ protein.

mined that the human γ_2, γ_3 and γ_4 cDNA clones expressed *in vitro*; it demonstrated the specificity of three anti-γ Abs, one generated to detect each of the three isoforms; it revealed that the stargazin-like γ_2, γ_3 and γ_4 all localize to the plasma membrane of COS-7 cells when expressed either alone or in combination with other VDCC subunits and finally it showed that COS-7 cells do not endogenously express γ_2, γ_3 or γ_4. Furthermore, because the anti-γ Abs, all of which were designed to detect epitopes in the C-terminus after the fourth predicted transmembrane segment, failed to stain COS-7 cells that had not been permeablized, it was established that the C-terminus is localized to the membrane and inside the cell. If predictions of secondary structure as envisaged by other laboratories are correct, a tetra-spanning transmembrane conformation will also place the N-terminus on the cytoplasmic side of the membrane [12,16].

The distribution of the γ_2, γ_3 and γ_4 in cerebellum

This study is the first immunohistochemical analysis of stargazin-like γ proteins in the human CNS. In the cerebellum, we observed that γ_2 was detected in molecular, granule and Purkinje cell layers as has been previously reported for mouse γ_2 protein [22] and mRNA [1,14,19]. A major difference between human and rodent immunostaining patterns was observed for γ_4, which was detected as very high levels in human cerebellar Purkinje cell bodies and processes, an observation not reported for rat or mouse [22,25]. The detection of γ_3 protein expression in the human cerebellum, albeit at extremely low levels, was similar to the γ_3 mRNA detection patterns reported in mouse or rat cerebellum [19,25] but disagree with the findings on our northern blots and the *in situ* hybridization data of Klugbauer et al. [14]. The positive, albeit weak detection of γ_3 protein in cerebellar interneurons and low levels detected in Purkinje cell bodies suggests that γ_3 is

expressed in distinct types of neurons in human cerebellum at levels too low to be detected by some hybridization conditions.

The almost inverse staining patterns of γ_2 and γ_4 in the dentate cerebellar nucleus (DCN) was striking. Much of the perisomatic neuropil surrounding the DCN somata consists of afferents from the Purkinje cells and is stained particularly strongly for γ_4 while the DCN cell bodies stained strongly for γ_2 but were devoid of γ_4 staining. It is therefore a reasonable assumption that γ_4 is pre-synaptically localized in the Purkinje cell afferents to the DCN whilst γ_2 localizes to the post-synaptic regions of the DCN cell bodies. Indeed this observation holds with the finding that γ_4 expressed well throughout Purkinje cell processes. γ_4 also appears to be localized in the GABAergic neurons of the cerebellum more than the excitatory glutamatergic cell types. In addition to showing strong immunostaining throughout Purkinje cells, γ_4 is detected in the interneurons of the molecular layer and also the Golgi interneurons of the granule layer. Whilst γ_2 is also detected in all these cell types, the γ_4 immunostaining is noticeably lower, if not absent from the excitatory granule cells, and is absent from the DCN cell bodies.

The distribution of γ_2, γ_3 and γ_4 in hippocampus

This study has determined that γ_2, γ_3 and γ_4 show differential but overlapping expression patterns in the human hippocampus and dentate gyrus. As is the case for the cerebellum, the expression patterns of γ_2 and γ_4 more closely resemble one another than that of γ_3. The γ_2, and γ_4 proteins were detected throughout the hippocampus and dentate gyrus, although there were variations in the staining of cell bodies, dendrites and neuropil in the different sub-fields. γ_3 localized more specifically in the neuronal cell bodies of the hippocampus and dentate gyrus. This possibly indicates that γ_2 and γ_4 are involved in synaptic modulation of neurotransmission throughout the cell, whereas γ_3 is solely involved in functions such as regulation of VDCCs or AMPA receptors in the cell soma.

$Ca_V2.1/\beta_4$ VDCC currents are not modulated by human γ_2 or γ_4 co-expression in the presence or absence of an $\alpha 2\delta_2$ subunit

The co-expression of γ_2 or γ_4 with $Ca_V2.1/\beta_4$ VDCCs in the absence or presence of the $\alpha 2\delta_2$ subunit, did not significantly affect peak current amplitude or any of the activation or inactivation properties. These data agree closely with the findings of Chen et al. [19] who recorded whole cell Ca^{2+} currents from *stg* and wild type cerebellar granule cells. They reported that absence of γ_2 neither altered the I-V relationship of the native whole cell Ca^{2+} current nor did it significantly modulate the steady-state inactivation properties of VDCC current compared to wild type. Although they did not use pharmacological agents to isolate specific components of the whole cell Ca^{2+} current which might have highlighted subtle changes particular to the P/Q-, N-, R-, or L-type currents present in this cell type [39,40], it is unlikely that another known γ isoform could functionally substitute for γ_2 to maintain normal VDCC function in that instance because distribution studies have shown that they are probably not expressed in this cell type [14,19,25]. This indicated that even if γ_2 was associated directly or indirectly with a VDCC complex in cerebellar granule cells [20,22], it did not modulate the high voltage activated VDCC I-V relationship or inactivation properties.

More recent patch clamp recordings from *stg* thalamic relay neurons showed a 45% increase in HVA VDCC peak current densities compared to wild type [21] consistent with a previous report that γ_2 inhibited high voltage activated VDCC peak current amplitude by 37–40% when expressed in *Xenopus* oocytes [20]. Why our data and those of Chen *et al*. [19] are so different from these results may be explained by differences in subunit combinations expressed in granule cells and thalamic relay neurons and between the two *in vitro* studies. Stargazin-like proteins might be able to directly modulate VDCC complexes consisting of particular subunit combinations, but are unable to reproduce this influence on other subunit complexes if they required additional interacting proteins not present in the *Xenopus* oocyte or cerebellar granule cells. The electrophysiological data therefore cannot be used as a strong argument to warrant considering these γ proteins as an integral part of high voltage-activated Ca^{2+} channels because modulation of current properties has not been reproducible between different studies. Nevertheless, there is biochemical evidence for the association of γ_2 and γ_3 with the N-type $Ca_V2.2$ channel [20,22] and it is quite possible that whilst γ_2, γ_3 and γ_4 readily associate with certain neuronal VDCC complexes, specific environmental conditions must be met for them to exert a measurable biophysical influence.

Conclusions

Human γ_2, γ_3 and γ_4 stargazin-like proteins (or TARPs) are detected solely in the CNS. On the whole, their differential distributions closely parallel those of their rodent orthologues as observed by northern blot, *in situ* hybridization, western blot and immunohistochemistry [1,14,19,22,25] with some notable exceptions. The differential expression pattern of each isoform among the cell types present in human cerebellum and hippocampus predicts specific roles for each subtype in neuronal function, and possibly even segregated VDCC-γ or AMPA receptor-γ complexes [25]. The results of our electrophysiology experiments support the notion that γ_2, γ_3 and γ_4 stargazin-like proteins are not "subunits" of VDCCs in the true sense of the word. Nevertheless, we do not discount

the possibility that they may interact with VDCCs and possibly influence trafficking, assembly or integration of VDCCs and AMPA-receptor function in their native environment or that to modulate VDCC current they require other factors not endogenously expressed in *Xenopus* oocytes.

Methods

cDNA sources and synthesis

Human brain total RNA was purchased from Invitrogen (Paisley, UK) and used to generate cDNA using the Superscript Pre-amplification System (Invitrogen) primed with random hexamers according to the manufacturer's instructions.

Isolation and cloning of the γ_2, γ_3 and γ_4 cDNAs

The complete open reading frame (ORF) of human *CACNG2* cDNA was amplified from 25 ng human brain cDNA by PCR (cycling parameters: 98°C for 1 min, then 30 cycles of 98°C for 30 s, 55°C for 30 s, 72°C for 2 min, followed by a final 10 min extension step at 72°C) containing Pfu polymerase and 25 pmol each of the gene specific primers (GSPs), 5'-GCGGCCGCACCATGGGGCTGTTTGATC-3' and 5'-GCTAGCCTCGAGTTAGTGTTTATATAATGAAGAA-3'. These amplify the ORF of *CACNG2*, with a 5' extension of a *Not* I restriction site and partial Kozak sequence for initiation of translation in vertebrates (ACC) [41] and a 3' extension of *Xho* I and *Nhe* I restriction enzyme sites. Amplified fragments of the correct size were purified from agarose gels using the Qiaex II kit (Qiagen, Crawley, UK), and cloned into pCR2.1-TOPO vector (Invitrogen). Positive colonies identified by blue/white screening were confirmed by *EcoR* I restriction digest of purified plasmid and were sequenced on both strands using T7 (5'-TAATACGACTCACTAT AGGG-3') and M13R (5'-CAGGAAACAGCTATGAC-3') universal primers and gene specific primers in an automated dye terminator sequencer (Applied Biosystems, Warrington, UK).

The same procedures used to clone human *CACNG2* were followed to clone *CACNG3* and *CACNG4*, but using the primer pairs, 5'-CGGCCGCCACCATGAGGATGTGTGACAGAGGTA-3' and 5'-GCTAGCCTCGAGTCAGTTCAGACGGGCGTGG TG-3' to amplify *CACNG3* ORF or, 5'-GCGGCCGCACCATGGTGCGATGCGACCGCG-3' and 5'-GCTAGCCTCGAGTCACACAGGGGTCGTCCGTC-3' to amplify *CACNG4* ORF. These primer pairs contained the same restriction enzyme sites and if appropriate, the partial Kozak sequence [41] in their 5' extensions as were included in the *CACNG2* primers. The human γ_2, γ_3, and γ_4 cDNAs were subcloned into the pMT2 vector for expression in *Xenopus* oocytes and COS-7 cells [42].

Other cDNA clones

The following cDNAs were used: rabbit $Ca_V2.1$ (X57689), rat β_4 (LO2315) and mouse $\alpha 2\delta_2$ (AF247139, common brain splice variant). All cDNAs were subcloned into expression vector pMT2 [42].

Antibodies

Multiple sequence alignments and basic local alignment search tool (BLAST) searches compared the protein sequences of all known stargazin-like γ proteins with one another and with other proteins in the public databases. This identified regions of lowest homology between γ_2, γ_3 and γ_4 that were not present in any other known proteins. The following peptides, TARATDYLQASAITRIPS (γ_2, amino acids 211–228), FHNSTPKEFKESLHNNPAN (γ_3, amino acids 291–309) and VHDFFQQDLKEGFHVSMLN (γ_4, amino acids 303–321), were synthesized by standard solid-phase techniques at Severn Biotech (Kidderminster, UK) to generate specific polyclonal antibodies (Abs). Each was coupled to the carrier protein tuberculin purified protein derivative (PPD) using sulpho- Succinimidyl4- [N-maleimidomethyl] cyclohexane-1-carboxylate (SMCC) (Pierce, Tattenhall, UK) via a Cys residue added at the N-terminus during synthesis. To raise polyclonal anti-γ_2, anti-γ_3 and anti-γ_4 Abs, the resulting conjugates were used to immunize Bacille Calmette-Guerin (BCG)-sensitized Dutch rabbits at monthly intervals [43]. The immune response was monitored by indirect enzyme-linked immunoabsorbent assay (ELISA) with free peptide-coated micro-titer plates. Immunoglobulins from the terminal bleeds were purified using immobilized peptide antigen columns (Sulfo-link, Pierce). Each anti-γ Ab was checked for specificity for its target by immunocytochemistry. COS-7 cells transfected with a single stargazin-like γ protein cDNA were examined for positive staining following incubation with the appropriate affinity purified Ab. Control slides were also examined for cross-reaction of the primary Ab with non-transfected COS-7 cells, stargazin-like γ proteins other than the target against which the primary Ab was intended to bind (data not shown) and the VDCC α_1, α2δ, and β subunits used in this investigation. Finally, positive staining of target protein was abolished following overnight pre-incubation (at 4°C) of the primary Ab with a 10 × molar excess of the peptide against which it was raised (data not shown).

Cell culture and transfections

COS-7 cell were cultured as previously described [44]. Transfection was performed using the Geneporter transfection reagent (Gene Therapy Systems, San Diego, CA). Cells were plated onto coverslips 2–3 h prior to transfection. The DNA and Geneporter reagent (2 μg and 10 μl, respectively) were each diluted in 500 μl of serum-free medium, mixed, and applied to the cells. The α_1, β, α2δ and γ cDNAs were mixed and transfected in a 1:1:1:1 ratio

by DNA weight. If a particular cDNA was absent from the transfection, substitution with blank pMT2 vector maintained correct subunit ratios. After 3.5 h, 1 ml of medium containing 20% serum was added to the cells, which were then incubated at 37°C for 3 days. Prior to staining, cells were re-plated using a non-enzymatic cell dissociation solution (Sigma, Dorset, UK) and maintained at 27°C for between 2 and 6 h.

Immunocytochemistry

COS-7 cells were fixed and permeablized for immunocytochemistry essentially as previously described [44]. Primary Abs, affinity purified anti-γ_2, anti-γ_3 and anti-γ_4 were used at 0.2 μg/ml. Secondary biotin conjugated or goat anti-rabbit (Sigma, Dorset, UK) Ab was applied at 5 μg/ml. Texas red-conjugated streptavidin was applied at 3.3 μg/ml. The nuclear dye 4', 6-diamidino-2-phenylindole (DAPI, 300 nM, Molecular Probes) was also used to visualize the nucleus. Cells were examined on a confocal scanning laser microscope (Leica TCS SP, Milton Keynes, UK). All images were scanned sequentially to eliminate cross-talk and photomultiplier settings kept constant in each experiment.

Northern blots

Human 12-lane multiple tissue blots and brain II and III blots (BD Biosciences Clontech) were hybridized at 65° C in ExpressHyb solution (BD Biosciences Clontech) according to the manufacturer's instructions. The [α^{32}P] radiolabeled γ probes corresponding to nucleotides 597–814, 560–792 or 594–804 of the γ_2, γ_3 or γ_4 ORFs respectively, were assembled according to the Strip-EZ DNA Probe Synthesis Removal Kit (Ambion (Europe) Ltd, Huntingdon, UK). The final stringency wash performed was 0.1 × Saline Sodium Citrate, 0.1% Sodium dodecylsulphate (SDS) at 65°C.

Human Brain Immunohistochemistry

Human brain tissue was obtained from two males aged 76 and 80 years whose causes of death were listed as metastatic carcinoma and left ventricular failure respectively. No prior history of brain disease was noted. The tissue, provided by the Cambridge Brain Bank Laboratory at the University of Cambridge, U.K., was collected using ethical consent procedures according to U.K. law. Sections were fixed in neutral buffered formalin and processed to paraffin wax. Paraffin-embedded wax blocks were sectioned on a Microm HM3555S microtome at 7 μm and underwent a microwave antigen retrieval procedure using a citrate buffer at pH 6.0 prior to immunostaining [45,46]. Endogenous peroxidase was blocked with 3% hydrogen peroxide in water followed by non-specific protein blocking in 5% milk powder in phosphate buffered saline (PBS). Sections were incubated overnight with primary Ab (anti-γ_2, 0.85 μg/ml; anti-γ_3, 1.3 μg/ml; anti-γ_4, 0.85 μg/ml) diluted with 3% goat serum and 0.1% Triton X-100 at 4°C in a moist chamber. Treatment of all sections post application of primary Ab was identical. Goat anti-rabbit (1:20 dilution, Biogenex, Wokingham, UK) link Ab was applied to all sections and incubated at room temperature for 20 min, followed by horseradish peroxidase-conjugated streptavidin (Biogenex, prediluted (1/20)) that was incubated for a further 20 min. Sections were visualized using 3,3'-diaminobenzidine (DAB) solution made up according to Vector kit SK-4100 (Peterborough, UK), and incubated with the sections for 2–10 min. In a few cases, sections were counterstained briefly in Mayer's hematoxylin prior to microscopic examination.

Negative control preparations performed in all immunohistochemistry experiments included replacement of primary antibodies with PBS only and preincubation of primary antibodies with the 100 μM corresponding immunizing peptide overnight at 4°C prior to immunostaining.

Microscopy and image analysis

Slides were analyzed using a Zeiss Axioplan Optical Microscope (Carl Zeiss Ltd., Welwyn Garden City, UK). All sections were viewed under bright-field illumination using × 2.5, × 10, × 20, or × 40 objectives and a stabilized light source. For each tissue section, both The Central Nervous System [47], and The Human Brain: an introduction to its functional anatomy [48] were used for reference, together with corresponding counterstained sections to locate and define nuclear groups. A JVC KY-F55B television camera attached to the microscope and a PC running AcQuis image capture software (Syncroscopy, Cambridge, UK) was used to obtain images of each section.

Electrophysiology

Adult female *Xenopus laevis* were killed by anesthetic overdose in a 0.25% solution of tricaine, decapitated, and pithed. Oocytes were removed and defolliculated by treatment with 2 mg/ml collagenase type IA in Ca^{2+}-free ND96 saline containing (in mM): NaCl, 96; KCl, 2; $MgCl_2$, 1; and HEPES, 5, pH-adjusted to 7.4 with NaOH for 2 hr at 21°C. Plasmid cDNAs for the different VDCC subunits were mixed in a weight ratio of 1:1:1:1, and ~10 nl was injected into the nuclei of stage V or VI oocytes. In control oocytes without a γ cDNA or in the absence of an α2δ cDNA, an equal volume of water was substituted in the mix. Injected oocytes were incubated at 18°C for 3–5 days in ND96 saline (as above plus 1.8 mM $CaCl_2$) supplemented with 100 μg/ml penicillin, 100 IU/ml streptomycin (Invitrogen), and 2.5 mM Na pyruvate. Whole-cell recordings from oocytes were made in the two-electrode voltage-clamp configuration under continuous gravity-fed superfusion (~1 ml/min) with a chloride-free solution

containing (in mM): $Ba(OH)_2$, 10; TEA-OH, 80; NaOH, 25; CsOH, 2; and HEPES, 5 (pH7.4 with methanesulfonic acid). In all experiments, oocytes were injected with 30–40 nl of a 100 mM solution of K3-1, 2-bis (aminophenoxy) ethane-N, N, N', N'-tetra-acetic acid (BAPTA) in order to suppress endogenous Ca^{2+}-activated Cl^- currents. Recording microelectrodes, were pulled from thick-walled borosilicate glass capillary tubing with the following dimensions: 1.5 mm outer diameter, 1.0 mm bore diameter and with an internal 0.1 mm fiber (Plowden and Thompson, Stourbridge, UK). The TEVC pipettes were pulled using a P-87 Flaming/Brown microelectrode puller (Sutter Instrument Company, Novato, CA). Electrodes contained 3M KCl and had resistances of 0.3–2 MΩ. The holding potential (V_H) was -100 mV. Membrane currents were recorded, amplified, low-pass filtered at 1 kHz using a Geneclamp 500 B amplifier, digitized through a Digidata 1200 interface (Axon Instruments, Foster City, CA) and stored on a PC using data acquisition software pClamp 6.02 (Axon Instruments). In all cases currents were leak subtracted on-line by a P/4 protocol. Additional analyses including calculation of means, standard error of the mean (S. E. M.), significance (unpaired Student's *t*-tests, where applicable) and curve fitting were calculated using Origin 5.0 (OriginLab Corporation, Northampton, MA). One-way analysis of variance (ANOVA) and post-hoc tests were performed using software available at http://faculty.vassar.edu/lowry/VassarStats.htm. Where mean values are presented they are shown as mean ± S. E. M. (with *n* depicting the number of oocytes from which the mean was calculated). Statistical significance was defined as $P < 0.05$.

Current-voltage (I-V) relation curves generated from currents activated by a 200 ms long depolarizing pulse were fitted with a combined Boltzmann and linear fit function:

$$I = G_{max} (V - V_{rev}) / (1 + \exp(- (V - V_{50act}) / k))$$

where I is the whole cell current amplitude, G_{max} is the maximum slope conductance, $V_{0.5act}$ is voltage of the mid-point of activation, V_{rev} is the reversal potential and k is the slope factor for activation.

Steady-state inactivation data were generated from currents activated by a 100 ms long depolarizing pulse from the holding potential (V_H) to 0 mV immediately after a 25 s conditioning pre-pulse between -100 and 0 mV. Current amplitudes were normalized to the maximum amplitude and fitted with a Boltzmann function of the form:

$$I / I_{max} = 1 / (1 + \exp((V - V_{50inact}) / k))$$

where I / I_{max} is the normalized peak current, $V_{50inact}$ is the voltage for the mid-point of inactivation, V is the conditioning voltage and k is the slope factor for inactivation.

Authors' contributions

FJM carried out the cloning of the human γ_2, γ_3 and γ_4 proteins, performed all the necessary practical and analytical procedures to acquire and process the primary data presented in this paper and drafted the manuscript. ACD and JJC participated in the conception, design and coordination of the study. All authors read and approved the final manuscript.

Acknowledgements

The Medical Research Council as part of an industrial collaborative PhD studentship with GlaxoSmithKline supported F. J. M. The Wellcome Trust provided additional support. The authors would like to thank Dr M. Rees (University College London) for the $\alpha 2\delta_2$ cDNA and acknowledge the assistance of Dr. Carles Cantì (University College London), and Dr. Chris Plumpton, Michael Hurle and Margaret Flint (GlaxoSmithKline, Stevenage, UK).

References

1. Letts VA, Felix R, Biddlecome GH, Arikkath J, Mahaffey CL, Valenzuela A, Bartlett F. S., 2nd, Mori Y, Campbell KP and Frankel WN: **The mouse stargazer gene encodes a neuronal Ca^{2+}channel γ subunit.** *Nat Genet* 1998, **19:**340-347.
2. Catterall WA: **Structure and regulation of voltage-gated Ca^{2+} channels.** *Annu Rev Cell Dev Biol* 2000, **16:**521-555.
3. Jay SD, Ellis SB, McCue AF, Williams ME, Vedvick TS, Harpold MM and Campbell KP: **Primary structure of the γ subunit of the DHP-sensitive calcium channel from skeletal muscle.** *Science* 1990, **248:**490-492.
4. Powers PA, Liu S, Hogan K and Gregg RG: **Molecular characterization of the gene encoding the γ subunit of the human skeletal muscle 1,4-dihydropyridine-sensitive Ca^{2+} channel (CACNLG), cDNA sequence, gene structure, and chromosomal location.** *J Biol Chem* 1993, **268:**9275-9279.
5. Bosse E, Regulla S, Biel M, Ruth P, Meyer HE, Flockerzi V and Hofmann F: **The cDNA and deduced amino acid sequence of the γ subunit of the L-type calcium channel from rabbit skeletal muscle.** *FEBS Lett* 1990, **267:**153-156.
6. Ahern CA, Powers PA, Biddlecome GH, Roethe L, Vallejo P, Mortenson L, Strube C, Campbell KP, Coronado R and Gregg RG: **Modulation of L-type Ca^{2+} current but not activation of Ca^{2+} release by the gamma1 subunit of the dihydropyridine receptor of skeletal muscle.** *BMC Physiol* 2001, **1:**8.
7. Freise D, Held B, Wissenbach U, Pfeifer A, Trost C, Himmerkus N, Schweig U, Freichel M, Biel M, Hofmann F, Hoth M and Flockerzi V: **Absence of the γ subunit of the skeletal muscle dihydropyridine receptor increases L-type Ca^{2+} currents and alters channel inactivation properties.** *J Biol Chem* 2000, **275:**14476-14481.
8. McEnery MW, Snowman AM, Sharp AH, Adams ME and Snyder SH: **Purified omega-conotoxin GVIA receptor of rat brain resembles a dihydropyridine-sensitive L-type calcium channel.** *Proc Natl Acad Sci U S A* 1991, **88:**11095-11099.
9. Ahlijanian MK, Westenbroek RE and Catterall WA: **Subunit structure and localization of dihydropyridine-sensitive calcium channels in mammalian brain, spinal cord, and retina.** *Neuron* 1990, **4:**819-832.
10. Liu H, De Waard M, Scott VE, Gurnett CA, Lennon VA and Campbell KP: **Identification of three subunits of the high affinity ω-conotoxin MVIIC-sensitive Ca^{2+} channel.** *J Biol Chem* 1996, **271:**13804-13810.
11. Martin-Moutot N, Leveque C, Sato K, Kato R, Takahashi M and Seagar M: **Properties of ω conotoxin MVIIC receptors associated with α1A calcium channel subunits in rat brain.** *FEBS Lett* 1995, **366:**21-25.

12. Black J. L., 3rd and Lennon VA: **Identification and cloning of putative human neuronal voltage-gated calcium channel γ-2 and γ-3 subunits: neurologic implications.** *Mayo Clin Proc* 1999, **74:**357-361.
13. Chu PJ, Robertson HM and Best PM: **Calcium channel γ subunits provide insights into the evolution of this gene family.** *Gene* 2001, **280:**37-48.
14. Klugbauer N, Dai S, Specht V, Lacinova L, Marais E, Bohn G and Hofmann F: **A family of γ-like calcium channel subunits.** *FEBS Lett* 2000, **470:**189-197.
15. Moss FJ, Viard P, Davies A, Bertaso F, Page KM, Graham A, Canti C, Plumpton M, Plumpton C, Clare JJ and Dolphin AC: **The novel product of a five-exon stargazin-related gene abolishes $Ca_V2.2$ calcium channel expression.** *Embo J* 2002, **21:**1514-1523.
16. Burgess DL, Davis CF, Gefrides LA and Noebels JL: **Identification of three novel Ca^{2+} channel γ subunit genes reveals molecular diversification by tandem and chromosome duplication.** *Genome Res* 1999, **9:**1204-1213.
17. Burgess DL, Gefrides LA, Foreman PJ and Noebels JL: **A cluster of three novel Ca^{2+} channel γ subunit genes on chromosome 19q13.4: evolution and expression profile of the γ subunit gene family.** *Genomics* 2001, **71:**339-350.
18. Rousset M, Cens T, Restituito S, Barrere C, Black J. L., 3rd, McEnery MW and Charnet P: **Functional roles of γ2, γ3 and γ4, three new Ca^{2+} channel subunits, in P/Q-type Ca^{2+} channel expressed in Xenopus oocytes.** *J Physiol* 2001, **532:**583-593.
19. Chen L, Chetkovich DM, Petralia RS, Sweeney NT, Kawasaki Y, Wenthold RJ, Bredt DS and Nicoll RA: **Stargazin regulates synaptic targeting of AMPA receptors by two distinct mechanisms.** *Nature* 2000, **408:**936-943.
20. Kang MG, Chen CC, Felix R, Letts VA, Frankel WN, Mori Y and Campbell KP: **Biochemical and biophysical evidence for γ2 subunit association with neuronal voltage-activated Ca^{2+} channels.** *J Biol Chem* 2001, **276:**32917-32924.
21. Zhang Yi, Mori Mayra, Burgess Daniel L. and Noebels Jeffrey L.: **Mutations in High-Voltage-Activated Calcium Channel Genes Stimulate Low-Voltage-Activated Currents in Mouse Thalamic Relay Neurons.** *J Neurosci* 2002, **22:**6362-6371.
22. Sharp AH, Black J. L., 3rd, Dubel SJ, Sundarraj S, Shen JP, Yunker AM, Copeland TD and McEnery MW: **Biochemical and anatomical evidence for specialized voltage-dependent calcium channel γ isoform expression in the epileptic and ataxic mouse, stargazer.** *Neuroscience* 2001, **105:**599-617.
23. Chetkovich Dane M., Chen Lu, Stocker Timothy J., Nicoll Roger A. and Bredt David S.: **Phosphorylation of the Postsynaptic Density-95 (PSD-95)/Discs Large/Zona Occludens-1 Binding Site of Stargazin Regulates Binding to PSD-95 and Synaptic Targeting of AMPA Receptors.** *J Neurosci* 2002, **22:**5791-5796.
24. Choi J, Ko J, Park E, Lee JR, Yoon J, Lim S and Kim E: **Phosphorylation of stargazin by protein kinase A regulates its interaction with PSD-95.** *J Biol Chem* 2002, **277:**12359-12363.
25. Tomita Susumu, Chen Lu, Kawasaki Yoshimi, Petralia Ronald S., Wenthold Robert J., Nicoll Roger A. and Bredt David S.: **Functional studies and distribution define a family of transmembrane AMPA receptor regulatory proteins.** *J Cell Biol* 2003, **161:**805-816.
26. Arikkath J, Chen CC, Ahern C, Allamand V, Flanagan JD, Coronado R, Gregg RG and Campbell KP: **γ1 subunit interactions within the skeletal muscle L-type voltage-gated calcium channels.** *J Biol Chem* 2003, **278:**1212-1219.
27. Schnell Eric, Sizemore Max, Karimzadegan Siavash, Chen Lu, Bredt David S. and Nicoll Roger A.: **Direct interactions between PSD-95 and stargazin control synaptic AMPA receptor number.** *PNAS* 2002, **99:**13902-13907.
28. Hashimoto K, Fukaya M, Qiao X, Sakimura K, Watanabe M and Kano M: **Impairment of AMPA receptor function in cerebellar granule cells of ataxic mutant mouse stargazer.** *J Neurosci* 1999, **19:**6027-6036.
29. Chen L, Bao S, Qiao X and Thompson RF: **Impaired cerebellar synapse maturation in waggler, a mutant mouse with a disrupted neuronal calcium channel γ subunit.** *Proc Natl Acad Sci U S A* 1999, **96:**12132-12137.
30. Mouritzen Dam A: **The density of neurons in the human hippocampus.** *Neuropathol Appl Neurobiol* 1979, **5:**249-264.
31. Volsen SG, Day NC, McCormack AL, Smith W, Craig PJ, Beattie R, Ince PG, Shaw PJ, Ellis SB, Gillespie A and et al.: **The expression of neuronal voltage-dependent calcium channels in human cerebellum.** *Brain Res Mol Brain Res* 1995, **34:**271-282.
32. Volsen SG, Day NC, McCormack AL, Smith W, Craig PJ, Beattie RE, Smith D, Ince PG, Shaw PJ, Ellis SB, Mayne N, Burnett JP, Gillespie A and Harpold MM: **The expression of voltage-dependent calcium channel β subunits in human cerebellum.** *Neuroscience* 1997, **80:**161-174.
33. Craig PJ, McAinsh AD, McCormack AL, Smith W, Beattie RE, Priestley JV, Yip JL, Averill S, Longbottom ER and Volsen SG: **Distribution of the voltage-dependent calcium channel α_{1A} subunit throughout the mature rat brain and its relationship to neurotransmitter pathways.** *J Comp Neurol* 1998, **397:**251-267.
34. Westenbroek RE, Sakurai T, Elliott EM, Hell JW, Starr TV, Snutch TP and Catterall WA: **Immunochemical identification and subcellular distribution of the α1A subunits of brain calcium channels.** *J Neurosci* 1995, **15:**6403-6418.
35. Tanaka O, Sakagami H and Kondo H: **Localization of mRNAs of voltage-dependent Ca^{2+}channels: four subtypes of α1- and β-subunits in developing and mature rat brain.** *Brain Res Mol Brain Res* 1995, **30:**1-16.
36. Stea A, Tomlinson WJ, Soong TW, Bourinet E, Dubel SJ, Vincent SR and Snutch TP: **Localization and functional properties of a rat brain α1A calcium channel reflect similarities to neuronal Q- and P-type channels.** *Proc Natl Acad Sci U S A* 1994, **91:**10576-10580.
37. Hobom M, Dai S, Marais E, Lacinova L, Hofmann F and Klugbauer N: **Neuronal distribution and functional characterization of the calcium channel α-2 subunit.** *Eur J Neurosci* 2000, **12:**1217-1226.
38. Barclay J, Balaguero N, Mione M, Ackerman SL, Letts VA, Brodbeck J, Canti C, Meir A, Page KM, Kusumi K, Perez-Reyes E, Lander ES, Frankel WN, Gardiner RM, Dolphin AC and Rees M: **Ducky mouse phenotype of epilepsy and ataxia is associated with mutations in the Cacna2d2 gene and decreased calcium channel current in cerebellar Purkinje cells.** *J Neurosci* 2001, **21:**6095-6104.
39. Randall A and Tsien RW: **Pharmacological dissection of multiple types of Ca^{2+} channel currents in rat cerebellar granule neurons.** *J Neurosci* 1995, **15:**2995-3012.
40. Pearson HA, Sutton KG, Scott RH and Dolphin AC: **Characterization of Ca^{2+} channel currents in cultured rat cerebellar granule neurones.** *J Physiol* 1995, **482 (Pt 3):**493-509.
41. Kozak M: **An analysis of 5'-noncoding sequences from 699 vertebrate messenger RNAs.** *Nucleic Acids Res* 1987, **15:**8125-8148.
42. Swick AG, Janicot M, Cheneval-Kastelic T, McLenithan JC and Lane MD: **Promoter-cDNA-directed heterologous protein expression in Xenopus laevis oocytes.** *Proc Natl Acad Sci U S A* 1992, **89:**1812-1816.
43. Lachmann PJ, Strangeways L, Vyakarnam A and Evan G: **Raising antibodies by coupling peptides to PPD and immunizing BCG-sensitized animals.** *Ciba Found Symp* 1986, **119:**25-57.
44. Brice NL, Berrow NS, Campbell V, Page KM, Brickley K, Tedder I and Dolphin AC: **Importance of the different β subunits in the membrane expression of the α1A and α2 calcium channel subunits: studies using a depolarization-sensitive α1A antibody.** *Eur J Neurosci* 1997, **9:**749-759.
45. McKee PH, Hobbs C and Hall PA: **Antigen retrieval by microwave irradiation lowers immunohistological detection thresholds.** *Histopathology* 1993, **23:**377-379.
46. Shi SR, Key ME and Kalra KL: **Antigen retrieval in formalin-fixed, paraffin-embedded tissues: an enhancement method for immunohistochemical staining based on microwave oven heating of tissue sections.** *J Histochem Cytochem* 1991, **39:**741-748.
47. Brodal Per: **The Central Nervous System.** 2ndth edition. *Oxford, Oxford University Press*; 1998.
48. Nolte J: **The Human Brain: an introduction to its functional anatomy.** 5thth edition. *London, Mosby*; 2001.